Nuclear Instruments and Methods in Physics Research B59/60 (1991) 344–352
North-Holland

Section IV. Beam-induced crystallization and amorphization

Structural relaxation in amorphous silicon and the role of network defects

S. Roorda, J.S. Custer and W.C. Sinke [1]
FOM Institute for Atomic and Molecular Physics, Kruislaan 407, 1098 SJ Amsterdam, Netherlands

J.M. Poate, D.C. Jacobson and A. Polman [2]
AT&T Bell Laboratories, 600 Mountain Avenue, Murray Hill, NJ 07974-2070, USA

F. Spaepen
Harvard University, Cambridge, MA 02138, USA

Structural relaxation of amorphous Si (a-Si) can be viewed as either a general network rearrangement (short range ordering) or as the analogue in a-Si of defect annihilation processes in crystal Si (c-Si). Some recent experimental results are discussed in the light of these two alternatives. The annealing kinetics of ion bombardment damage in a-Si and c-Si are remarkably similar. The solubility of Cu in a-Si decreases with annealing, whereas the diffusivity increases which suggests removal of trapping sites (defects) from the material as relaxation proceeds. These phenomena can be understood when it is assumed that structural relaxation of a-Si is fully controlled by annihilation of point defects. The defect density in fully unrelaxed a-Si is estimated to correspond to several at.% displaced atoms. The absence of a measurable densification upon structural relaxation of a-Si suggests mutual annihilation of low- and high-density defects.

1. Introduction

Most physical properties of amorphous silicon (a-Si) have long been known to depend on the thermal history of the material. Examples are the optical, vibrational, structural, and thermodynamic properties as probed by infrared analysis [1], Raman spectroscopy [2], X-ray diffraction [3], and differential scanning calorimetry (DSC) [4,5], respectively. These thermally induced changes are known as "structural relaxation" (SR) because they involve continuous relaxation of the structure to a state of lower free energy. Since it is firmly established that considerable changes can occur in the atomic structure of the a-Si network, we will now try to establish the physical mechanism of SR. There are two different scenarios which can be summarized as follows.

1) In the first approach [6,7], SR is thought to be accomplished by an overall change in the topology of the (fourfold coordinated covalently bonded) network. That is, every atom contributes to SR by small local changes leading to a smaller average bond angle distortion and smaller stored strain energy in the network. These kind of changes are also known as short range ordering (SRO), and have no analogue in crystal Si (c-Si) because c-Si has long range order.

2) In the second approach [8] it is recognized that the network is likely to contain a large number of nonequilibrium defects. We use the term network defect for any defect that may occur in a random network. Possible candidates are dangling or floating bonds, unique for the amorphous network, or (di-, tri-, etc.) vacancy and interstitial type defects similar to those in c-Si. These defects may conglomerate and/or annihilate, as in fact has been inferred from electron spin resonance (ESR) [9] and luminescence measurements [10]. It remains to be established, however, what the importance of defect annealing is in the process of SR, and whether the processes envisioned in the two scenarios 1 and 2, are mutually exclusive or intimately related. In addition, a relation may exist between SR in pure a-Si and defect-related phenomena in hydrogenated a-Si (a-Si : H) [11].

In this article we will examine some recent experiments in light of this problem. It will be shown that SR in a-Si can be understood as annihilation of a large number of point defects, similar to the mechanism of radiation damage recovery in c-Si. It appears that the

[1] Present address: Netherlands Energy Research Foundation, ECN, P.O. Box 1, 1755 ZG Petten, Netherlands.
[2] Present address: FOM Institute for Atomic and Molecular Physics, Kruislaan 407, 1098 SJ Amsterdam, Netherlands.

0168-583X/91/$03.50

defect densities estimated on the basis of ESR are several orders of magnitude lower than indicated by a combination of ion scattering and DSC results. The actual defect densities in unrelaxed a-Si are expected to be so high that every atom feels the presence of a defect in its immediate surrounding.

2. Densification and structural relaxation

2.1. Density measurements

Since the early days of a-Si research, it has been known that the atomic density of a-Si is less than that of the crystal [12]. However, all recent computer modeling studies find a-Si densities which are higher than that of the crystal [13]. Here we are not only concerned with the density itself but with the *increase* in the a-Si density induced by thermal annealing. Such densification has been observed in a-Si prepared by deposition [12,14]. It has long been thought to be an essential ingredient of SR because it accompanies changes in the vibrational density-of-states and the X-ray diffraction pattern. That this is not the case was demonstrated recently by accurate measurements of the density of a-Si prepared by ion implantation by Custer et al. [15].

By implanting (at 77 K) through a steel contact mask Custer et al. prepared a finger pattern of ion implanted a-Si on the surface of a c-Si wafer. Since the a-Si fingers are laterally confined, a difference in density between a-Si and c-Si shows up as a physical step at the edge of each finger. By measuring the step height with an Alphastep and the total amount of a-Si by ion channeling the relative densities of a-Si and c-Si have been accurately determined. Fig. 1 shows the step height for layers of different thickness [15]. The open symbols correspond to as-implanted a-Si which did not receive any thermal treatment. The solid symbols correspond to a-Si layers which received a thermal treatment at temperatures of up to 580°C. Least-squares linear fits to the data yields the density differences between as-implanted a-Si and annealed a-Si on the one hand and c-Si on the other of $1.79 \pm 0.13\%$ and $1.70 \pm 0.07\%$, respectively. These values are the same within the experimental accuracy and it is concluded therefore

1) that the atomic density of a-Si is $1.74 \pm 0.06\%$ less than that of c-Si and
2) that a-Si prepared by ion implantation cannot be densified significantly even though DSC and X-ray diffraction show unambiguously that the material can be structurally relaxed.

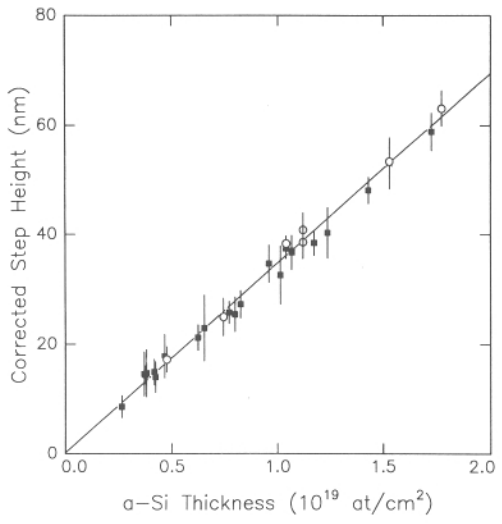

Fig. 1. Physical step height for a-Si layers of different thickness relative to c-Si. Open symbols: as-implanted; solid symbols: thermally annealed at various temperatures (after Custer et al. [15]).

2.2. Implications for relaxation scenarios

These conclusions have some important implications. All computer models of a random network [13] (except the original hand-built model by Polk [16]) calculate a higher density of a-Si as compared to that of the crystal. The experimental observation (in void-free material) of the opposite indicates an essential ingredient is missing in the computer modeling. One such ingredient could be to model a system which contains a large concentration of a variety of network defects.

Measurements of the density of a-Si prepared deposition techniques generally yield large density deficits. It seems that these deficits have to be attributed to the presence of macroscopic voids in the network. Densification, therefore, is in fact removal of these voids and does not affect the network density. This conclusion is corroborated by the observation of rapid diffusion through a connected void network in deposited a-Si [17] and the increase in the average coordination number upon densification of sputtered a-Si [14]. In addition, changes in the ESR signal induced by thermal annealing of deposited a-Si have been attributed to void coalescence. In a-Si which contains macroscopic density deficits, SR and densification may occur simultaneously but should be considered as separate processes.

The fact that the density does not change significantly with SR puts some limits on the physical processes associated with it. Coming back to the two scenarios for SR sketched in the introduction these limits are as follows. For scenario 1 where SR is seen as an overall change in average network parameters it means that the average bond length and coordination number must remain virtually unchanged (it seems less plausible that the changes in bond length and coordination have opposite effects on the density). For the

second approach, 2, where SR is thought to be mediated by defect annihilation it means that the most probable scheme is that of mutual annihilation of high- and low-density type defects. The simplest example of such a mechanism is interstitial-vacancy recombination (although it should be kept in mind that in c-Si both single interstitials and vacancies are already mobile at very low temperatures [18]).

3. Relaxation and displacement damage

We will now try to distinguish between the two scenarios for SR. The strategy will be to compare SR with formation and annealing of (ion beam induced) displacement damage in both c-Si and a-Si. The comparison will consist of results from differential scanning calorimetry (DSC), Raman spectroscopy, and (in section 4) of measurements of impurity diffusion and solubility. For most details concerning the experimental procedures we refer to several recent publications [3,8,19,20].

Amorphous Si was prepared in a relaxed state by thermal annealing at 500°C. These well relaxed a-Si samples were then bombarded (at 77 K) with either He, C, Si, or Ge ions. Some c-Si samples were simultaneously subjected to identical treatments. Energies ranged from 50 keV to 8.3 MeV and fluences from 10^{11} to 10^{17} cm^{-2}. The dose is expressed as displacements per atom (dpa), by multiplying the ion dose with the number of target atomic displacements per incident ion in the region of interest and dividing by the number of target atoms in the same region. The number of target atom displacements is estimated from Monte Carlo simulations [21] and the region of interest is a 100 nm thick surface layer for Raman measurements and a 2 μm thick layer for DSC measurements.

3.1. Calorimetry of displacement damage

Fig. 2 shows the DSC signal from c-Si (bottom) and well relaxed a-Si (top), both after He bombardment to a dose of 0.3 dpa ("0.3 dpa Si"). The top trace has been offset. In the DSC figures a positive signal corresponds to a heat release during the first time the material is heated with a constant temperature increment of 40 K/min. The dashed line indicates the zero-signal baseline. The trace for a-Si exhibits a sharp peak near 690°C which is due to crystallization. This peak is clearly absent on the curve for c-Si. The shape of the peak is determined by the crystallization kinetics: crystallization occurs via solid phase epitaxial regrowth at the a-Si/c-Si interface which is thermally activated with a single activation energy of 2.7 eV [22]. Therefore the heat flow increases exponentially with temperature until all a-Si has crystallized.

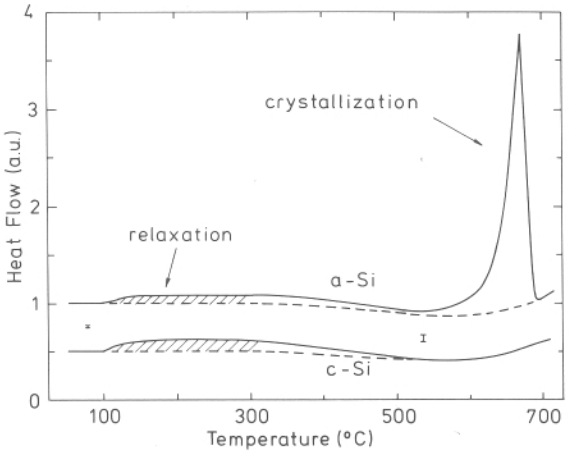

Fig. 2. DSC traces for relaxed a-Si (top) and c-Si (bottom), after bombardment with He^+ ions to a fluence resulting in 0.3 dpa (120 keV/2.1×10^{15} cm^{-2} and 200 keV/3.5×10^{15} cm^{-2}).

At low temperatures both curves show a heat release over a wide temperature range (hatched areas) without any peaks. This is attributed to removal of ion beam induced damage which is evidently not characterized by a single activation energy. Such a broad and featureless heat release is also characteristic of SR which already indicates that the kinetics of SR and ion-damage removal (in a-Si and c-Si) are similar. In order to study the low-temperature heat release in detail, DSC scans over a smaller temperature range were done which increases the baseline stability considerably. Before we discuss these results, it is useful to examine the ion damage in the c-Si samples.

Ion channeling (RBS) and transmission electron microscopy (TEM) have been used to characterize the ion beam induced damage in c-Si [8,19]. The results can be summarized as follows. For 0.03 and 0.1 dpa, only point defects are present (where we use the term "point defect" loosely, to include all defect clusters too small to be imaged in TEM), amounting to 5% displaced atoms in case of the 0.1 dpa bombardment as measured by RBS. The damage in the 0.3 dpa c-Si is mostly in the form of a high density of small amorphous zones, which are expected to be embedded in a background of lattice damage similar to that in 0.1 dpa c-Si. The total number of displaced atoms as measured by RBS amounted in this case to 20 at.%. The 1 dpa bombardments lead to the formation of a thick a-Si layer which extends almost completely to the surface. After DSC measurements to a maximum temperature of 400°C, all damage has disappeared, leaving a perfect crystal except in case of the 1 dpa bombardment (note that for one DSC measurement the samples are heated twice and are held at 400°C for a few minutes). We can now return to the low temperature heat release.

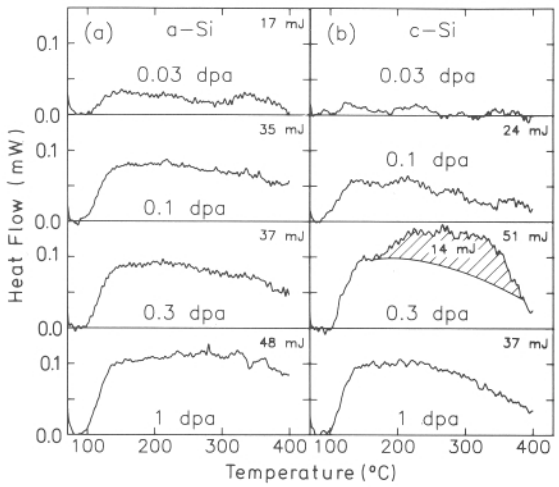

Fig. 3. Low-temperature DSC traces for (a) well relaxed a-Si and (b) c-Si, after bombardment with He^+ ions (50, 120, and 200 keV). The hatched area is discussed in the text.

In fig. 3 the low-temperature DSC traces of well relaxed a-Si (fig. 3a) and c-Si (fig. 3b) are shown after bombardment with He^+ ions to a range of ion fluences. The numbers in the right upper corner of each of the panels indicate the total heat released. The curves for less than 0.03 dpa did not differ significantly from the zero-signal baseline and are not shown. The curves for 0.03 to 1 dpa a-Si deviate clearly from the baseline and show a heat release similar to that observed when as-implanted a-Si is ramp heated for the first time. Saturation occurs between 0.03 and 0.1 dpa.

A clear heat release is observed from the 0.1 dpa implants in c-Si. This sample contains only damage in the form of point defects which anneals out during DSC to 400°C. We therefore conclude that the heat release from 0.1 dpa c-Si is due to annihilation of point defects alone. These point defects seem to anneal out continuously over a range of temperatures, as opposed to annealing kinetics dominated by only a few processes (which would give rise to peaks in the DSC trace). This implies a zoo of point defects in irradiated c-Si, with a large number of routes to annihilation. Combining the total heat released (25 mJ) with the measured number of displaced atoms gives an estimate of the average heat release per displaced atom of 0.6 eV.

The heat release from c-Si at 0.3 dpa is due to the removal of both point defects and amorphous zones. The low-temperature excess heat release (hatched area) can be understood in terms of recrystallization of amorphous zones at anomalously low temperatures (the anomalous shape of the DSC curve for 0.3 dpa c-Si is not visible in fig. 2; the sensitivity there is reduced because of the higher temperatures reached during that measurement). The assumption is made that the heat release is a linear superposition of annihilation of point defects (i.e. 0.6 eV/displaced atom) and heat release from crystallization of amorphous zones (0.12–0.16 eV/atom [3–5]). The hatched area in fig. 3 would then correspond to 13–10 at.% and the remaining area to 8 at.% displaced atoms, thus giving a total number of 21–18 at.%. This is in excellent agreement with the channeling estimate of 20 at.%. One possible reason for the low crystallization temperature of these small amorphous zones could be that they are embedded in a sea of defects which can enhance crystallization [23,24].

Comparison of the left and right side panels shows that the *shape* of all curves are very similar except that of 0.3 dpa c-Si which has just been attributed to low-temperature crystallization of amorphous zones. Moreover, not only are the *scanned* curves similar in shape, but also the *isothermal* decay curves of the heat release at the end temperature of each of the DSC curves are very similar [19]. It is concluded therefore that both the temperature dependence and the kinetics of SR and defect annihilation are very similar.

3.2. Implications for relaxation scenarios

If we now discuss these data in relation to the two scenarios for SR, we come to the following observations. A remarkable similarity in shape exists between the (identically bombarded) 0.1 dpa a- and c-Si curves and that of SR of a-Si (see the trace for 1 dpa c-Si). Contrary to expected in scenario 1, it appears that SR does have an analogue in c-Si, namely annihilation of a large population of point defects. Scenario 2, which states that defects play an important role, is fully consistent with the data. Not only does SR give rise to a similar DSC trace as point defect annihilation in 0.1 dpa c-Si, but also the DSC trace of 0.1 dpa a-Si has the same shape. Examination of the DSC data in the context of scenario 2 leads to the following analysis of the defect densities involved.

A rough estimate of the defect densities involved in SR can be made by comparing the stored energy per displaced atom in c-Si determined above (0.6 eV) with the integrated heat release from 0.03 and 0.1 dpa a-Si. Under the assumption that the average heat release from one annihilation event in a-Si is equal to that in c-Si, this yields 3.5 and 7.3 at.% displaced atoms in 0.03 and 0.1 dpa a-Si, respectively. These densities are not necessarily equal to the number of defects because several displaced atoms may form one defect complex. Furthermore, the analysis relies on an RBS measurement of the number of displaced atoms in 0.1 dpa c-Si, and the defects have been implicitly assumed to be homogeneously distributed throughout the implanted layer. Nevertheless, the agreement of this estimate with the Monte Carlo calculations (i.e. the calculated damage dose in dpa) is striking. Comparing this with the typical number for the decrease in spin density upon annealing

of a-Si prepared by ion implantation of 1×10^{19} cm^{-3} [9] (or 0.02 at.%, a factor of 200 less than above), it appears that a large majority of the defects cannot be detected by ESR. This is not unexpected since ESR is only sensitive to uncharged and unpaired dangling bonds while most dangling bonds are probably either charged or paired.

The saturated defect density in a-Si (i.e. 7.3 at.% displaced atoms) is close to the background point defect level (8 at.% displaced atoms) estimated above for 0.3 dpa c-Si. It appears that the intrinsic damage saturation level is similar in a- and c-Si and that in both cases the super-saturated Si collapses to unrelaxed a-Si. The reason that a somewhat lower ion dose is required to reach the same defect level in a-Si than in c-Si may indicate that defect formation processes are more efficient in the former. The observation that the defect saturation levels are the same in a- and c-Si relies on the assumption that the stored energy per defect is the same in both materials; the absolute value of the saturation level has to be taken with some reserve because the cross sections for direct scattering from point defects in RBS are unknown.

3.3. Raman spectroscopy of displacement damage

Raman spectroscopy is known to be a sensitive probe of the state of relaxation of a-Si, as is best seen from the width and position of the main peak in the a-Si Raman spectrum. Upon relaxation, the half-width at the high-frequency side ($\Gamma/2$) becomes smaller and the peak position (λ_0) shifts to higher values. These changes have been associated with a decrease in the average bond angle distortion in the a-Si network and are considered characteristic of increasing short range order as meant under scenario 1.

Fig. 4 shows $\Gamma/2$ (bottom) and λ_0 (top) as a function of ion dose for C^+, Si^+ and Ge^+ bombarded a-Si which had previously been thermally annealed (relaxed). The values for as-implanted and well relaxed a-Si are also indicated. The ion dose is expressed in dpa as well as in ions/cm^2. For low ion doses, $\Gamma/2$ and λ_0 resemble the values characteristic for well relaxed a-Si, while for high doses they resemble values of as-implanted a-Si. The transition from relaxed to unrelaxed occurs for ion doses on the order of ≈ 0.02 dpa, irrespective of the mass of the projectile.

When the three projectiles are compared on an equivalent dpa basis, the amount of energy deposited in a-Si due to electronic stopping changes over several orders of magnitude. Therefore it can be concluded that the phenomenon of derelaxation by ion beams is due to nuclear collisions. Since the major part of the transition has occurred for a dose of 0.05 dpa, it appears that only one out of every 20 Si atoms needs to be displaced by a violent collision in order to almost completely derelax

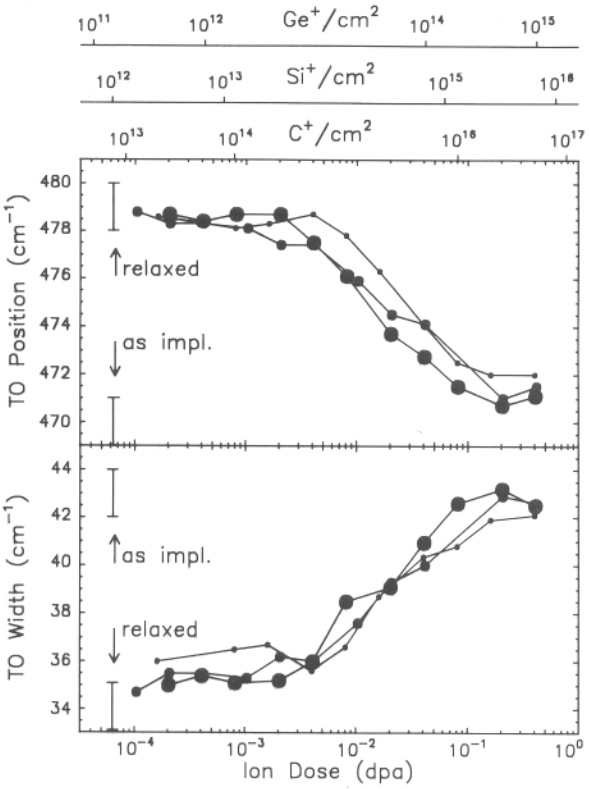

Fig. 4. Half-width (bottom) and position (top) of the TO-like Raman peak from annealed a-Si as a function of postanneal ion bombardment dose. Increasing symbol size corresponds to increasing projectile mass for C^+, Si^+ and Ge^+ ions.

the a-Si. This value is in good agreement with the damage saturation threshold in a-Si determined from the DSC measurements to be between 0.03 and 0.1 dpa (see fig. 3).

A similar scaling to equivalent dpa has been observed in the calorimetry experiments. The DSC traces shown in figs. 2 and 3 are obtained on He^+ bombarded material. Experiments with Si^+ and Ge^+ ion bombardments reproduced the results shown on figs. 3a and 3b, provided the ion fluences were scaled to dpa. This shows again that ion beam induced damage which gives rise to a heat release is due to nuclear collisions rather than electronic energy loss mechanisms.

Previous interpretations of the changes in the a-Si Raman spectrum due to SR have been solely in terms of average bond angle distortion $\Delta\Theta$ according to scenario 1. It is now seen that the introduction into relaxed a-Si of ion damage which is most likely in the form of point defects, is accompanied by similar changes in the Raman spectrum (but of opposite sign). In the next section we will try to solve this apparent contradiction.

3.4. Raman spectroscopy and calorimetry

The relation between the Raman peak width $\Gamma/2$ and the average bond angle distortion $\Delta\Theta$ can be tested experimentally. The test takes advantage of the fact that the stored enthalpy ΔH in a-Si is largely due to strain energy related with distorted bonds [25]. The two scenarios for SR described in the introduction each give rise to a different relation between ΔH and $\Gamma/2$.

1) For a Keating-type potential, the strain energy due to distorted bonds is roughly proportional to the square of $\Delta\Theta$. Because the Raman peak width in turn depends roughly linearly on $\Delta\Theta$, it follows that in scenario 1 a linear relation is expected between $\Gamma/2$ and the square root of the total stored enthalpy, $\sqrt{\Delta H}$ [6,7].

2) Alternatively, a linear relation between the stored strain energy and $\Gamma/2$ may be found. In scenario 2 it is assumed that a large concentration of complex point defects exists in a-Si and that these defects play an important role in SR. In general, point defects in Si are surrounded by small strained regions [18]. To a first approximation $\Delta\Theta$ will then be proportional to the relative volume of strained material. As long as strained regions do not overlap the volume of strained material will be proportional to the defect concentration. Thus $\Delta\Theta$ is a linear function of the number of point defects. Assuming that ΔH is the sum of the crystallization enthalpy ΔH_{cryst} and a relaxation enthalpy ΔH_{rel} proportional to the point defect concentration, a linear relation then exists between $\Delta\Theta$ and $\Delta H_{\text{rel}} = \Delta H - \Delta H_{\text{cryst}}$.

Using DSC, both ΔH and ΔH_{rel} have been determined for a-Si which was brought to different intermediate states of relaxation by thermal treatments at various temperatures (150–500°C), and these values have been compared with the Raman peak width [3,19]. In fig. 5a the square root of ΔH is shown while fig. 5b displays ΔH_{rel}. Solid lines represent linear least squares fits to the data points.

$$\sqrt{(\Delta H)} = 0.071(\Gamma/2 + 17.6), \tag{1}$$

where ΔH is measured in kJ/mol and $\Gamma/2$ in cm^{-1}. This experimentally established relation may be used to quantify the relations between $\Gamma/2$ and $\Delta\Theta$ and between $\Delta\Theta$ and ΔH. Assuming that the slope represents the ratio of $\sqrt{k_\Theta}$ (the bond bending force constant relating $\Delta\Theta$ to ΔH) over f (the proportionality constant between $\Gamma/2$ and $\Delta\Theta$), then either k_Θ should be smaller (by at most a factor of 0.63) or f larger (by at most a factor of 1.3) than previous estimates [6]. However, the offset also differs from the predicted value, indicating that another contribution to ΔH may exist.

In fig. 5b, the relation between ΔH_{rel} and $\Gamma/2$ is shown. The solid line is a linear least squares fit which describes the data reasonably well. In the simplified picture 2 sketched above, the slope of 0.6 kJ cm/mol would correspond to the ratio $H_{\text{def}}/(\Gamma_{\text{def}} V_{\text{def}})$. Here, H_{def} represents the (average) stored energy per defect (or defect cluster), Γ_{def} the local broadening in $\Gamma/2$ due to strained bonds in the neighbourhood of the defect, and V_{def} the volume of the strained region. It is observed that the fits of figs. 5a and 5b both describe the data points equally well. Consequently, neither of the aforementioned scenarios can be rejected on the basis of these results. It is emphasized that the relation found in fig. 5b relies on the same physical interpretation of the relation between Raman peak width and distorted bonds but with the extra ingredient that distorted bonds are localized in strained regions surrounding defects.

4. Displacement damage and impurity solubility

The study of solubility and diffusion (S&D) mechanisms can be a useful probe of the atomic structure of a

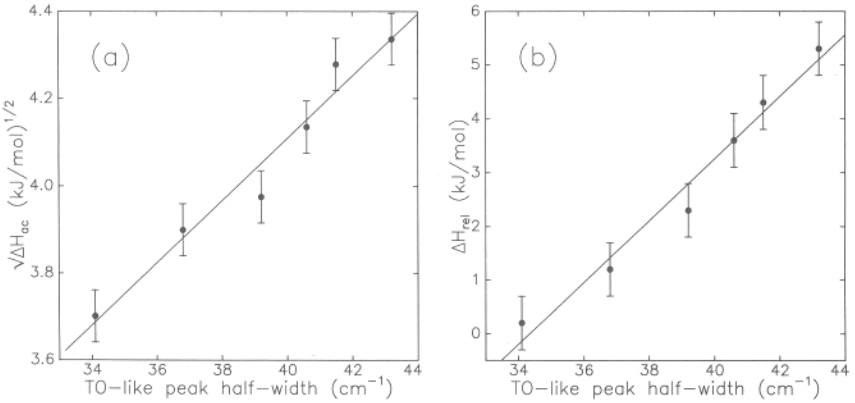

Fig. 5. Relation between $\Gamma/2$ and enthalpy difference for a-Si after a thermal anneal at temperatures up to 500°C. (a) Square root of ΔH_{ac} versus $\Gamma/2$, and (b) excess enthalpy ΔH_{rel} versus $\Gamma/2$. Solid lines represent least-squares linear fits to the data points.

solid. It has been established [26,27] that Cu, Ag, and Au are fast diffusors in a-Si and moreover that there is a remarkable correlation between diffusion in a- and c-Si in both absolute magnitude and activation energy. It can be generally stated [28] that the fast diffusers in c-Si, with interstitial components, are fast diffusers in a-Si and that the slow, substitutional diffusers in c-Si are also slow in a-Si. The solubility of fast diffusing species in a-Si was found to be at least six orders of magnitude greater than their solubility in c-Si. It is known that these species can be trapped or gettered at defects in c-Si, which means that the presence of defects in c-Si leads to a higher effective solubility. With this in mind, we will now examine the S&D behaviour of Cu in a-Si in different states of relaxation and relate it to the relaxation scenarios.

4.1. Measurements of Cu diffusion

Multiple implantation of MeV Si ions into c-Si was used to create a thick a-Si layer. The sample was cut into three pieces, two of which were annealed in vacuum for 1 h at 500°C. One of the annealed samples was then implanted with 5.5 MeV Si ions leading to 0.1 dpa over the entire a-Si layer [21]. This results in derelaxation of the a-Si surface layer as has been shown from the DSC and Raman results (section 3). All three samples were then implanted with 4×10^{15} ions/cm^2, 200 keV Cu ions. The ion beam damage (in the toplayer) resulting from this implant amounts to approximately 5 dpa. The diffusion behaviour of Cu in all samples was then studied following annealing at 221°C for 4 h. Cu concentration profiles before and after annealing were measured using RBS [20].

Fig. 6 shows backscattering spectra of all three samples before and after annealing at 221°C. The as-implanted Cu profile peaks at approximately 120 nm below the surface and the peak Cu concentration amounts to 0.55 at.%. After annealing of the unannealed sample significant in-diffusion of Cu is observed (fig. 6a). The typical diffusion distance is in agreement with parameters found in an earlier study [26].

An entirely different behaviour is observed in the "relaxed" sample (fig. 6b). A uniform Cu concentration is observed in an approximately 300 nm thick surface layer, and a low-concentration Cu tail is observed in the deeper lying relaxed layer. This tail extends deeper into the sample than the Cu diffusion profile in the unrelaxed sample and shows a rather constant Cu concentration over the depth range represented in the spectrum, indicating that the Cu diffusivity has increased considerably. The interface between the two concentration regions coincides with the end-of-range of the Cu implant (indicated by an arrow), and thus with the maximum depth to which the toplayer has been derelaxed. Fig. 6c shows the Cu diffusion profile in the "derelaxed" sample; it is essentially the same as that of the unrelaxed sample in fig. 6a.

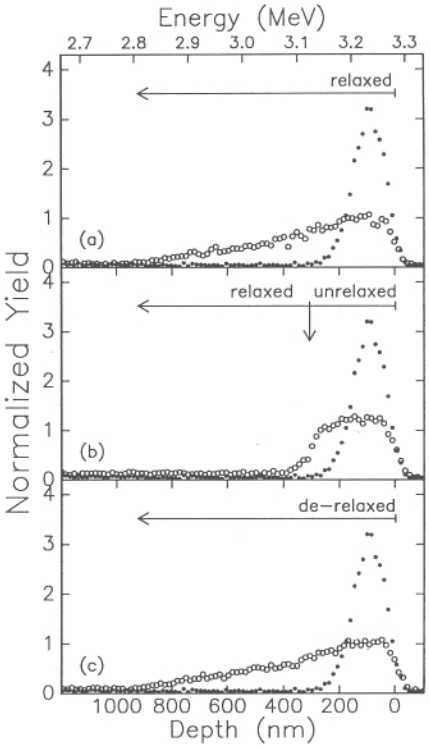

Fig. 6. Backscattering spectra of Cu implanted a-Si before (open circles) and after annealing at 221°C for 4 h (closed circles). (a) Unrelaxed, (b) double layer of relaxed and unrelaxed, (c) derelaxed a-Si.

4.2. Solubility, diffusion and relaxation scenarios

Scenario 1 for SR in terms of a general network rearrangement or short range ordering gives no clue as to how SR affects impurity behaviour. The situation becomes even worse when the effect of SR on diffusion in a-Si is compared with that in metallic glasses because in that case SR leads to a decrease in diffusivity [29] instead of an increase. Although the diffusion mechanism may be different it is not a priori clear why the effect of SR on diffusion should have opposite sign in a-Si and metallic glasses. Scenario 2 however views SR in a-Si as a defect mediated process which offers a simple explanation for both the diffusivity and solubility behaviour.

The discontinuity in the Cu concentration profile at the interface between the relaxed and unrelaxed materials is indicative for solute partitioning. This suggests that the effective solubility, or trap density, is different in the two structural states. The partition coefficient in fig. 6b is 9 ± 1, indicating that thermal annealing at 500°C for 1 h reduces the trap density by about an

order of magnitude. In additional experiments it was found that the partition coefficient is smaller when the a-Si is relaxed at lower temperatures which indicates that the trap density is a gradually decreasing function of annealing temperature.

The flat Cu tail in fig. 6b shows that Cu diffuses more rapidly in relaxed a-Si than in unrelaxed a-Si. More detailed measurements have shown that the difference in Cu diffusivity in the two structural states can amount to a factor of 2–5. According to scenario 2, relaxation of the a-Si network reduces the trap density, therefore the average distance between traps becomes larger and as a result a faster diffusion component becomes apparent.

Fig. 6c convincingly demonstrates the effect of an ion beam in derelaxing a-Si. Apparently 0.1 dpa is sufficient to derelax relaxed a-Si to a state which equals that of unrelaxed a-Si as far as Cu diffusion is involved. This supports the above interpretation of results from Raman spectroscopy and DSC experiments which show that 0.03 dpa is adequate to derelax a-Si. It also confirms the interpretation that defects or traps govern the S&D behaviour of Cu in a-Si.

5. Synopsis and conclusions

In summary, we have discussed several recent experiments concerning structural relaxation (SR) in amorphous Si (a-Si) in relation to two different scenarios for the physical mechanism of SR. Characterization of as-prepared, relaxed, and ion beam damaged a-Si by widely different techniques such as calorimetry, Raman spectroscopy, atomic density, impurity diffusion, and impurity solubility measurements have led to a range of experimental data. All results can be understood if it is assumed that SR is fully mediated by annihilation of network defects. A quantative analysis in this context yields an estimate for the average stored energy per displaced atom (as measured by RBS) of ≈ 0.6 eV in c-Si and a defect density in unrelaxed a-Si corresponding to several at.% displaced atoms.

The picture of SR in terms of annihilation of point defects (acting as traps for impuritues) is fully consistent with the observation that with SR, the solubility decreases and the diffusivity increases of Cu in a-Si. It is emphasized that this picture is not in conflict with earlier interpretations of changes in the Raman spectrum of a-Si. These changes can be easily well understood as being due to strained regions surrounding point defects in a relatively undistorted a-Si matrix. Combining the above estimate of the defect density with the size of these strained regions (assuming that only nearest and next-nearest neighbours are involved) shows that in unrelaxed a-Si every atom feels the presence of a defect in its immediate vicinity. This may be construed as an indication that point defect annihilation as proposed under scenario 2 is the underlying physical mechanism for the short range ordering processes envisioned in scenario 1.

Acknowledgements

Work at FOM was part of the research program of the Stichting voor Fundamenteel Onderzoek der Materie (FOM) and was made possible by financial support from the Nederlandse organisatie voor Wetenschappelijk Onderzoek (NWO) and the Stichting Technische Wetenschappen (STW). Work at Harvard was supported by the USA National Science Foundation through the Harvard Materials Research Laboratory under contract number DMR-86-14003.

References

[1] G.K. Hubler, E.P. Donovan, K.W. Wang and W.G. Spitzer, Soc. Photo-Optical Instr. Eng. 530 (1985) 222.
[2] W.C. Sinke, T. Warabisako, M. Miyao, T. Tokuyama, S. Roorda and F.W. Saris, J. Non-Cryst. Solids 99 (1988) 308.
[3] S. Roorda, W.C. Sinke, J.M. Poate, D.C. Jacobson, P. Fuoss, B.S. Dennis, S. Dierker and F. Spaepen, Mater. Res. Soc. Symp. Proc. 157 (1990) 683.
[4] S. Roorda, S. Doorn, W.C. Sinke, P.M.L.O. Scholte and E. van Loenen, Phys. Rev. Lett. 62 (1989) 1880.
[5] E.P. Donovan, F. Spaepen, J.M. Poate and D.C. Jacobson, Appl. Phys. Lett. 55 (1989) 1516.
[6] W.C. Sinke, S. Roorda and F.W. Saris, J. Mater. Res. 3 (1988) 1201.
[7] J.S. Lannin, Phys. Today 41 (1988) 28; J. Non-Cryst. Solids 97/98 (1987) 39.
[8] S. Roorda, W.C. Sinke, J.M. Poate, D.C. Jacobson, S. Dierker, B.S. Dennis and F. Spaepen, Appl. Phys. Lett. 56 (1990) 2097; Solid State Commun. 75 (1990) 197; Mater. Res. Soc. Symp. Proc. 157 (1990) 709.
[9] W.G. Spitzer, G.K. Hubler and T.A. Kennedy, Nucl. Instr. and Meth. 209/210 (1983) 309.
[10] R.A. Street, Adv. Phys. 30 (1981) 593.
[11] For recent reviews, see: H. Fritzsche (ed.), Amorphous Silicon and Related Materials, vols. 1A&B of Advances in Disordered Semiconductors (World Scientific, Singapore 1989).
[12] M.H. Brodsky, D. Kaplan and J.F. Ziegler, Appl. Phys. Lett. 21 (1972) 305.
[13] See, e.g.: F. Wooten, K. Winer and D. Weaire, Phys. Rev. Lett. 54 (1985) 1392;
R. Car and M. Parrinello, Phys. Rev. Lett. 60 (1988) 204;
T. Uda, Solid State Commun. 64 (1987) 837;
R. Biswas, G.S. Crest and C.M. Soukoulis, Phys. Rev. B36 (1987) 7473.
[14] J. Fortner and J.S. Lannin, Phys. Rev. B39 (1989) 5527.
[15] J.S. Custer, M.O. Thompson, D.C. Jacobson, J.M. Poate, S. Roorda, W.C. Sinke and F. Spaepen, Appl. Phys. Lett.

(in press); Mater. Res. Soc. Symp. Proc. 157 (1990) 689.
[16] D.E. Polk and D.S. Boudreaux, Phys. Rev. Lett. 31 (1973) 92.
[17] J.C. Bean and J.M. Poate, Appl. Phys. Lett. 36 (1980) 59.
[18] Point Defects in Solids, vol. 2, eds. J.H. Crawford and L.M. Slifkin (Plenum, New York, 1975) p 4.
[19] S. Roorda, W.C. Sinke, J.M. Poate, D.C. Jacobson, S. Dierker, B.S. Dennis, D.J. Eaglesham, F. Spaepen and P. Fuoss, submitted to Phys. Rev. B.
[20] A. Polman, D.C. Jacobson, S. Coffa, J.M. Poate, S. Roorda and W.C. Sinke, Appl. Phys. Lett. 57 (1990) 1230.
[21] Calculated using TRIM, a Monte Carlo simulation program;
J.P. Biersack and L.J. Haggmark, Nucl. Instr. and Meth. 174 (1980) 257;
J.F. Ziegler, J.P. Biersack and U. Littmark, The Stopping and Range of Ions in Solids (Pergamon, New York, 1985).
[22] G.L. Olson and J.A. Roth, Mater. Sci. Rep. 3 (1988) 1.
[23] K.A. Jackson, J. Mater. Res. 3 (1988) 1218.
[24] O.W. Holland, C.W. White, M.K. El-Ghor and J.D. Budai, J. Appl. Phys. 68 (1990) 2081.
[25] E.P. Donovan, F. Spaepen, D. Turnbull, J.M. Poate and D.C. Jacobson, J. Appl. Phys. 57 (1985) 1795.
[26] J.M. Poate, D.C. Jacobson, J.S. Williams, R.G. Elliman and D.O. Boerma, Nucl. Instr. and Meth. B19/20 (1987) 480.
[27] L. Calcagno, S.U. Campisano and S. Coffa, J. Appl. Phys. 66 (1989) 1874.
[28] J.M. Poate, D.C. Jacobson, F. Priolo and M.O. Thompson, Mater. Res. Soc. Symp. Proc. 128 (1989) 533.
[29] H.S. Chen, L.C. Kimerling, J.M. Poate and W.L. Brown, Appl. Phys. Lett. 32 (1978) 461.